

APPENDIX TO

SHEAR-WAVE SPLITTING PATTERNS IN PERACHORA (EASTERN GULF OF CORINTH, GREECE)

Ioannis Spingos¹, Vasilis Kapetanidis¹, Georgios Michas¹,
George Kaviris¹, Filippos Vallianatos^{1,2}

¹ Section of Geophysics – Geothermics, Department of Geology and Geoenvironment, National and Kapodistrian University of Athens, Athens, Greece

² Institute of Physics of Earth’s Interior and Geohazards, UNESCO Chair on Solid Earth Physics and Geohazards Risk Reduction, Hellenic Mediterranean University Research Center, Crete, Greece

Appendix A. Template-matching

To increase the number of events available for shear-wave splitting parameter determination, we applied a template-matching technique, by employing the open-source EQCorrscan code [Chamberlain et al., 2018]. This method takes advantage of the waveform similarity between groups of seismic events with identical source parameters to detect them, by scanning continuous waveform records, as well as pick their P- and S-wave arrival-times automatically.

We used the initial solutions for 828 manually analyzed events as templates. The preparation of data for the template matching method includes down-sampling to 50 Hz (from the original 100 Hz sampling rate), to reduce processing time, de-trending and filtering in a frequency band between 2 and 15 Hz, to reduce noise, while ensuring enough waveform complexity to distinguish between different multiplets. The P-waves are cropped on the vertical channel, while the S-waves are cropped on the two horizontal channels of each station with available data and positioned in a template by retaining their relative time delays, according to the differences in their arrival times. During the detection procedure, a normalized correlation coefficient is calculated for all available channels, considering these time delays.

We used the Median Absolute Deviation (MAD) as a measure of similarity, with a threshold value of 8. When the MAD value surpasses the threshold and is then maximized, the corresponding time is registered as a “detection” and the P and S arrival-times of the templates are imposed at the respective time of the best fit on the continuous records. In a next step, these detected arrival times are fine-tuned, by performing cross-correlation for each P or S-wave on each station separately, within a small Interval of time-lags around the initial detection time. This allows for some flexibility, as the detected event’s hypocenter may be slightly offset from that of the template, causing small differences in the respective travel-times.

The hypocenter of the template is imposed as a solution for each detection made using it. Accordingly, the origin time is estimated by subtracting the P- and S-wave travel-times of the template from the respective arrival-times of the detection. Finally, a “relative magnitude” is determined, in the form of a magnitude difference Δm , from the ratio of waveform amplitudes between a template and an associated detection, following the formula in Eq. (A1), similar to the one proposed by Schaff and Richards [2014]:

$$\Delta m = \log \frac{std(tr2)}{std(tr1)} + \log \frac{(1 + 1/snr_2^2)}{(1 + 1/snr_1^2)} \times CC \quad (A1)$$

where std is the standard deviation of the waveform amplitudes, $tr1$ and $tr2$ are the traces of the template and detection, respectively, with $snr1$ and $snr2$ the corresponding signal-to-noise ratio for template and detection, and CC is the correlation

coefficient. The difference Δm is subtracted from the known magnitude of the template to estimate the “relative” magnitude of the detected event. Finally, a search for duplicate detections is performed, as the same signal could be recognized by different templates belonging to the same multiplet. In such cases, the detection that provided the higher MAD value is retained.

From the above procedure, a total of 23,000 detections were made. In the context of the current study, template-matching was used as a means of increasing candidate event-station pairs for shear-wave splitting. Therefore, our main goal was to acquire arrivals even in single stations. However, due to the sparsity of the network, we identified cases of clear and impulsive detections at a single station (e.g. HP.LTK) that were noisy, missing or contaminated in others (i.e. in HA.LOUT and, especially, in HA.LTRS, which is equipped with a less sensitive accelerometer). As determining enough phases for locating the additional low-amplitude events anew was impossible, the fixed (relocated) hypocenters of the templates were used as the focal parameters.

To select arrivals suitable for SwS determination, we developed a station-centric and arrival-independent approach. Signal windows were cut 10 s before and 30 s after each detection. Then, after detrending and applying a 2-15 Hz bandpass filter, a modified SNR value was estimated according to Eq. (A2):

$$SNR_{mod} = \frac{\max|A_s|}{|A_n|} \quad (A2)$$

where A_s and A_n the normalized amplitudes in the signal and noise windows, respectively. The start of the noise window was set 5 s before the detection and the end of the signal window 15 s after. Then, the detections and their corresponding template were plotted and visually inspected to determine a satisfying modified SNR cutoff (Fig. A1). Finally, only detections with a modified SNR of at least 20 were considered for the SwS analysis, leading to 4,908 additional events. For

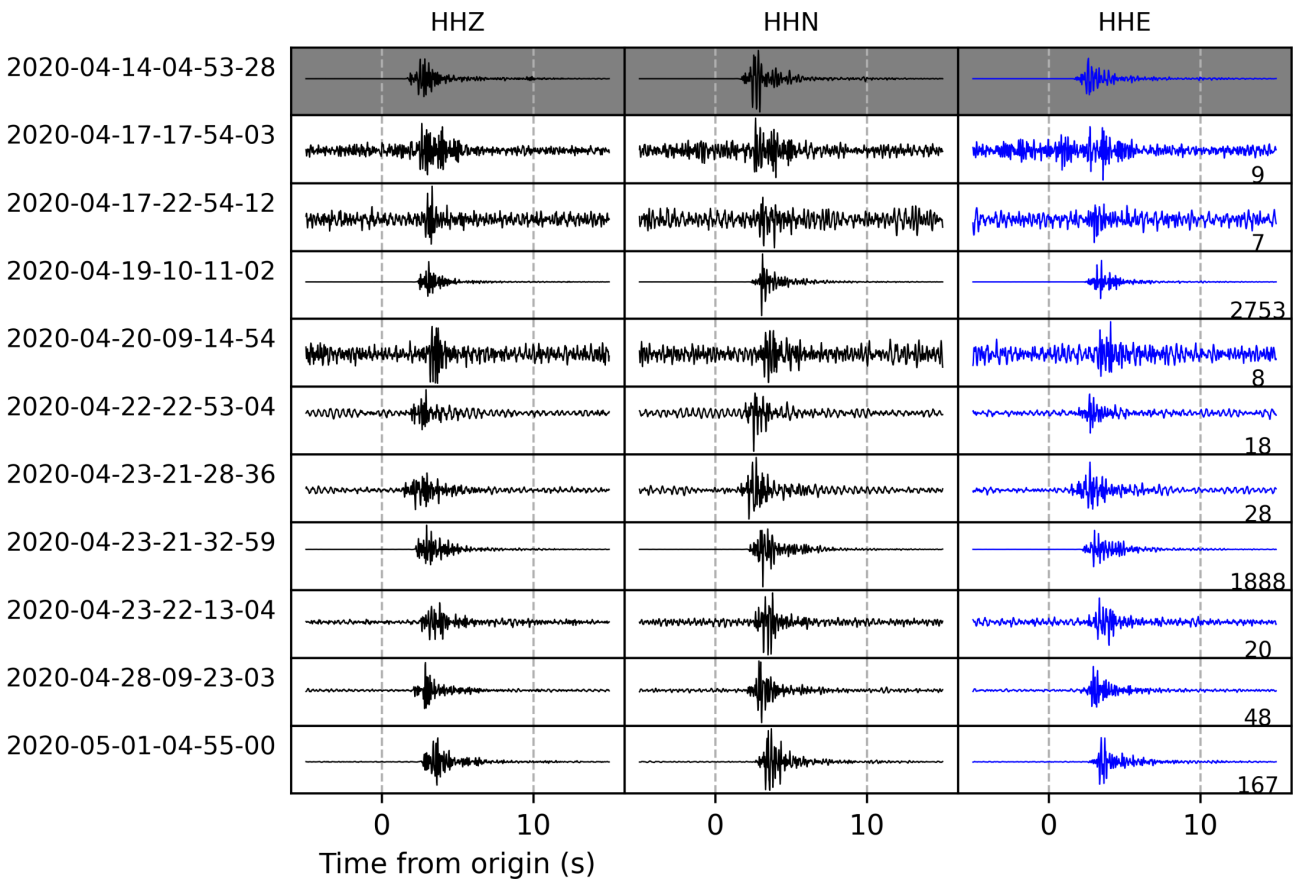


Figure A1. Plot of a template (top row, shaded traces) and corresponding detections (origin times shown at the left of each subplot), for the vertical (left column), north-south (middle) and east-west (right) channels at station HP.LTK. The modified SNR is shown at the bottom-right corner of each east-west diagram.

each detection, we used the travel time obtained from the related template to estimate the P- and S- arrivals. The fixed (relocated) hypocenters of the templates are used as the focal parameters of the associated detections, as their relative location errors are expected to be much smaller.

Appendix B. Shear-wave splitting analysis

The parameterization used in our study is provided in Table B1. The travel times for p and s waves were obtained from the catalog, with the exception of the automatically picked cases. The windowing scheme during the processing for splitting involves the automatic determination of the dominant period in the arriving shear-waves. The left end, before the arrival, of each candidate window is given by the $t_s - t_p$ time and a fixed value, while the right side of the windows are based on the estimated shear-wave period and a given value. Trial frequencies for the filters were decided after visually inspecting the spectra of a sample of recordings. We preferred wide ranges to avoid oversimplifying the signals and risk cycle-skipping.

Parameter	Value
Maximum time-delay	350 ms
Minimum SNR	1.5
Minimum T_s	0.1 s
Maximum T_s	2.0 s
Maximum $t_s - t_p$	1.5 s
Period factor (c_T)	3.0
Startpoints of signal windows	Between $(t_s - t_p)/2$ and 0.1 s, before the shear-wave arrival (step of 0.05 s)
Endpoints of signal windows	Between 0.1 s and $T_s * c_T$ after the shear-wave arrival
$C_{critical}$	3.2
Maximum number of clusters	10
Minimum number of points per cluster	5
Linkage criterion	Ward
Lower frequency filter corners (Hz)	0.5, 0.8, 1.0
Upper frequency filter corners (Hz)	8.0, 10.0, 20.0

Table B1. Parameterization for the shear-wave splitting analysis. T_s is the shear-wave period estimated by the software and t_p and t_s are the travel times for p and s waves, respectively.

In Fig. B1, an example of the processed event-station pairs is shown. The successful removal of anisotropy leads to a linearized particle motion diagram.

2015 – 05 – 06T02 : 56 : 58.630; HP. LTK EV
baz: 293.0N°E, **ain:** 42.3°, **epi:** 12.5 km **mag:** 1.4
 φ : 46.0 ± 2.3 N°E, **t_d :** 160.00 ± 0.97 ms, **p :** 118.8N°E, **grade:** A, **fit:** 0.5 | 8.0 Hz

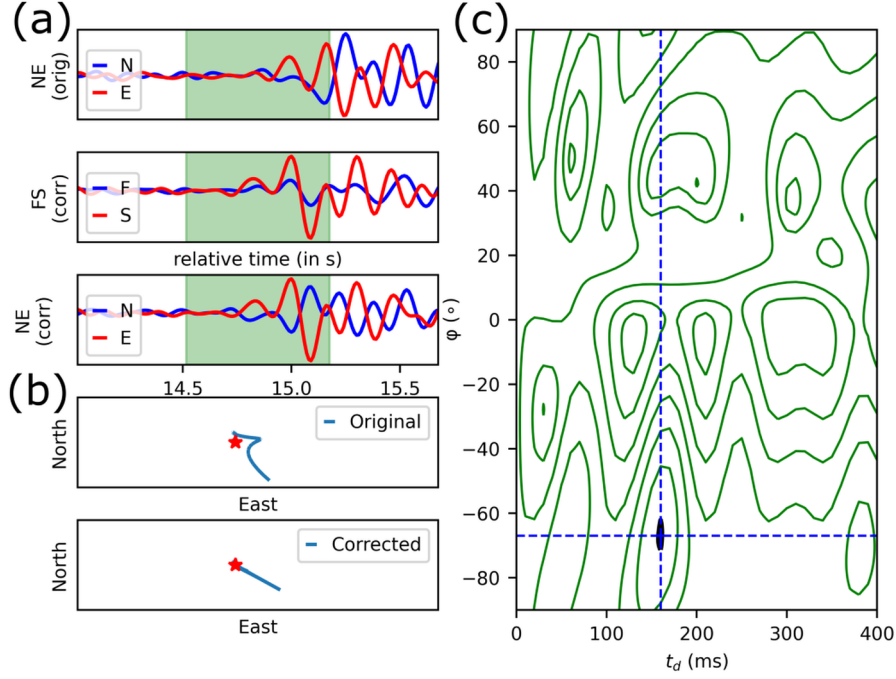


Figure B1. Shear-wave splitting measurement with the Eigenvalue (EV) method, on a window selected with cluster analysis (see Fig. B2). (a) Initial recordings of the horizontal channels (top), rotated to an axial system defined by φ (F) and its perpendicular direction (S) after correcting the time-delay (middle) and corrected for anisotropy (bottom), (b) particle motion diagram before (top) and after (bottom) correcting for anisotropy and (c) contour plot of the second eigenvalue λ_2 dependent of each splitting parameter pair. Basic information about the event-station pair is shown at the top. **baz**; the backazimuth, **ain**; the angle of incidence, **epi**; the epicentral distance (in km), **mag**; the magnitude, **fit**; the filter range used.

Selection of the window shown in Fig. B1 was carried out by the cluster analysis [Teauby et al., 2004] shown in Fig. B2. The algorithm recognized sub-clusters that would not be specified visually by the user.

The parameters used for the automatically grading of the splitting results are presented in Table B2. The null criterion refers to the difference between φ and the final polarization p obtained from the waveforms, after correcting for anisotropy. In other words, if the S_{fast} polarization is either (sub)parallel or (sub)perpendicular to the corrected particle motion, we are unable to reliably assess anisotropy, therefore the measurement is considered as a null. Grading scores are the upper threshold for each qualitative score. Observations with a score higher than that of “D”, are marked as “E”. For more information about the grading algorithm and its modular nature, see Spingos et al. [2020].

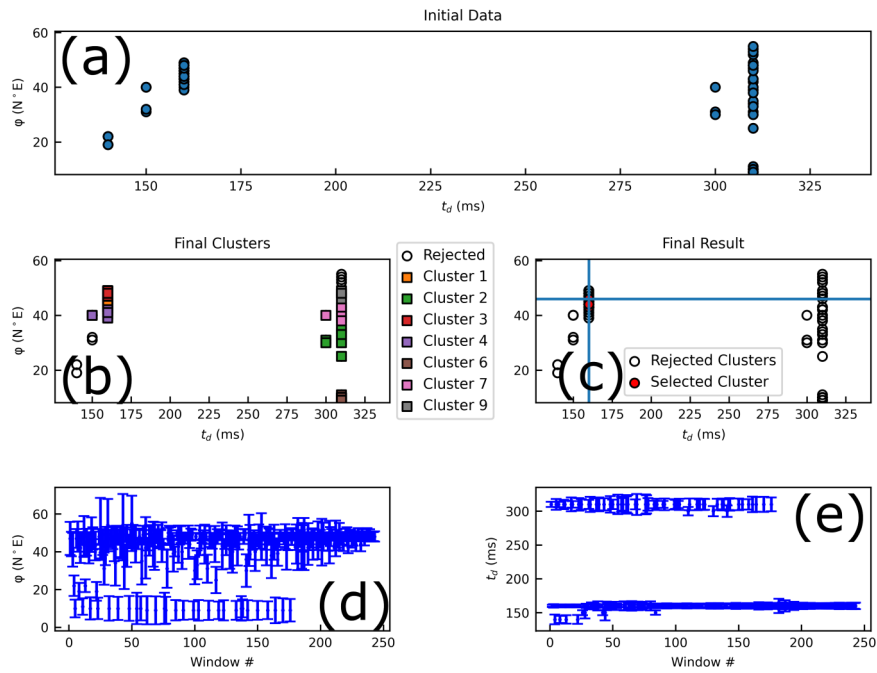


Figure B2. Example of cluster analysis results, based on which the signal window used in Fig. B1 was selected. (a) Initial space defined by ϕ and t_d , (b) initial clustering, (c) selection of the optimal cluster, (d) variation of ϕ per trial signal window and (e) variation of t_d per signal window.

Parameter	Value
Maximum accepted ϕ error	10°
Maximum accepted t_d error	10.0 ms
Correlation Coefficient in the FS system	0.60
Correlation Coefficient in the NE system	0.60
Null criterion	10° or 0 ms
Maximum "A" score	0.25
Maximum "B" score	0.50
Maximum "C" score	0.75
Maximum "D" score	1.00

Table B2. Grading parameters.

Appendix C. Null measurements

A total of 40 observations were characterized as null, i.e. with φ being either sub-parallel or sub-perpendicular to the corrected shear-wave polarization p [Wüstefeld and Bokermann, 2007]. We also checked for cases of null time-delays, but there were none in the dataset (even though Pytheas tries for $t_d = 0$ ms when performing the grid search in the eigenvalue method). All observations were made at HP.LTK, with an average φ of $N70^\circ E$ and a standard deviation of 27° . Distribution of φ shows significant scatter, with a preferential NE-SW orientation and a modest E-W concentration (Fig. C1a). Time-delays ranged between 70 and 350 ms (the latter being the boundary imposed by user criteria), with most being well over 100 ms (Fig. C1b). The average t_d from null observations is 207 ms with a standard deviation of 73 ms. Only 7 null measurements belong in the 2008-2019 era, with the majority (33) of them being determined by events belonging to 2020.

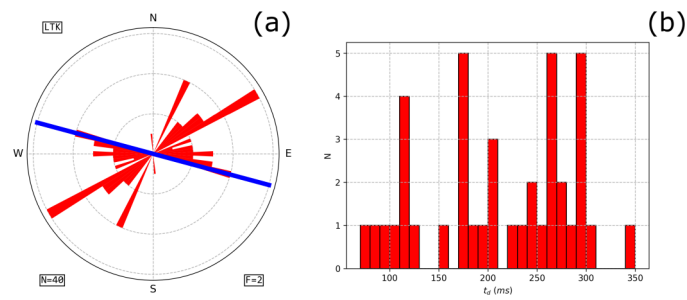


Figure C1. (a) Rose diagrams for null measurements at HP.LTK. Angles are binned every 5° . F indicates the interval of the grid. The black line shows the mean direction of φ at each station, as acquired from accepted measurements (graded A, B or C). (b) Distribution of t_d obtained from null measurements at HP.LTK.